THE ANNALS OF "DUNAREA DE JOS" UNIVERSITY OF GALATI
FASCICLE V, TECHNOLOGIES IN MACHINE BUILDING,
ISSN 2668-4829 (PRINT) 2668-4888 (ONLINE)
https://doi.org/10.35219/tmb.2025.1.06

A REVIEW OF IMAGE PROCESSING FOR DETECTING AND ANALYSING TRANSMISSION ERROR IN GEARS

Mihai-Cătălin RADU[1], Gabriel ANDREI[1]

[1] Mechanical Engineering Department, Faculty of Engineering, "Dunarea de Jos" University of Galati, Romania
email: mihai.radu@ugal.ro

ABSTRACT

Transmission error (TE) of gear pairs is the main cause of gear vibration and noise. Over the last few years, non-contact optical and vision-based techniques have developed in conjunction with present image processing, point cloud analysis, and machine learning to enable direct, high-resolution assessment of tooth profiles and surfaces appropriate for TE estimates and diagnostic monitoring. Acquisition modalities, image processing pipelines, mathematical techniques for TE computation or profile extraction, and validation criteria are all summarised in this paper.

KEYWORDS: transmission error, image processing, gear vibration.

1. INTRODUCTION

The instantaneous difference between the output gear's actual angular position and the angular position it would have under the same input rotation if the gears were perfectly conjugate (ideal involute kinematics) is commonly referred to as transmission error (TE) [1,2]. As a function of the input/output rotation angle θ, TE(θ) is usually expressed in arc-minutes or microradians. TE plays a crucial role in the design of high-performance gears and in quality control, as it is a primary contributor to gear noise and vibration (NVH) [3].

Miura and Nakamura [4] assert that when the maximum phase difference resulting from gear meshing errors coincides with the edge of the engine's vibrational revolution, a separation occurs between the crankshaft and camshaft of the gear teeth. An excessive relative velocity leads to impact actions. Research indicates that enhancing the macro geometry of gear teeth can effectively reduce noise. There are two primary connections between image processing and tooth meshing (TE). Firstly, the geometric approach utilizes point clouds, 3D optical scanning, and 2D profile extraction to accurately evaluate tooth geometry (including profile, lead, tip/trench, and flank) [5]. Secondly, it involves the identification and quantification of defects (such as pitting, spalling, fractures, plastic deformation, and wear) that modify local contact conditions and stiffness, subsequently affecting local TE signatures and dynamic responses. Vision systems that analyze the area, density, and dispersion of pitting yield data for dynamic models that correlate faults with variations in TE [6].

Traditional TE measurements are conducted through mechanical means (single-flank composite tests, double-flank testing) or by utilizing encoders or accelerometers under stress. Optical and image-based techniques enable TE estimation from measured geometry (whether noisy or loaded) and enhance the spatial localization of the error source, providing direct and comprehensive geometric data of tooth profiles and surfaces [7].

For inspections related to surface pitting, missing teeth, scratches, and contours on manufacturing lines, standard 2D imaging (utilizing telecentric lenses to minimize distortion, along with ring lights and bright/dark field illumination) remains widely used. While 2D imaging is efficient and cost-effective, it falls short in measuring depth or 3D profile variations that contribute to TE. Recent advancements aim to improve measurement precision by integrating subpixel edge detection with meticulous illumination [8].

Dense point clouds of tooth flanks are generated through laser and structured light triangulation techniques. By simulating meshing contact based on observed geometry, these point clouds facilitate virtual TE calculations and comprehensive surface deviation maps. Recent studies have demonstrated that virtual TE extraction using optical point clouds can either complement or replace traditional encoder-based TE measurements [5].

Studies focusing on stress and strain concentrations along, as well as on the onset of micro-damage that may anticipate TE development, can benefit from the evaluation of sub-micron surface displacements and small deformation fields. These quantities can be measured using digital holographic interferometry and other full-field coherent optical techniques. Although these techniques are more specialized, they are particularly effective for contact mechanics research and diverse TE experiments [9].

2. ANALITYCAL METHODS FOR DETERMINING TRANSMISSION ERROR IN GEARS

2.1. Definition

Kinematic models based on pure rolling translate involute geometry and pitch inaccuracies into relative displacement during the meshing process. In the case of ideal involute gears, the transmission error (TE) is nonexistent when there are no profile or pitch errors, misalignment, elastic deformation, or dynamic effects [10].

A gear pair's TE equation along the whole line of action may be expressed as follows [11]:

$$TE(t) = r_p\theta_p(t) + r_g\theta_g(t), \quad (1)$$

where r_p and r_g stand for the base circle radii, and θ_p and θ_g are the pinion and gear rotational displacements.

Transmission error can be considered as a minimised objective function. The dynamics equation of motion can be written as follows [12]:

$$\begin{aligned} &m_e x''(t) + c(x'(t) - e'(t)) + k(t) f_1(x(t) - \\ &-e(t)) + k_{bs}(t) f_2(x(t) - e(t)) = T_g(t), \end{aligned} \quad (2)$$

where T_g is the equivalent applied load, m_e is the equivalent mass, c is the constant mesh damping. k(t) represents the time-varying mesh stiffness function in direct contact, and $k_{bs}(t)$ forms the time-varying mesh stiffness function in backside contact. The DTE (dynamic transmission error) is highlighted by the function x(t). The backlash function is represented by f(t), while the manufacturing error is represented by e(t). The current TE is expressed as x(t) - e(t).

2.2 Profile deviation and TE

A first-order approximation of geometric TE is as follows: if the instantaneous contact point is at $x_c(\phi)$ and a measured tooth profile deviation (from nominal involute) is $\Delta(x)$ assessed along the flank coordinate x (e.g., normal direction along profile) [13]:

$$TE_{geomc}(\phi) \approx \Delta_1(x_c(\phi)) + \Delta_2(x'_c(\phi)), \quad (3)$$

where Δ_1, Δ_2 are deviations on the wheel and pinion, respectively, and x_c and x'_c maps the pair's contact geometry maps the pair's contact geometry.

The mapping is integrated across several simultaneous contact locations with weighting by contact influence functions in thorough tooth contact analysis, producing a convolutional integral form:

$$TE_{geom}(\phi) = \int cw(\xi;\phi)\Delta(\xi)d\xi, \quad (4)$$

with $w(\xi;\phi)$ representing an influence (sensitivity) kernel that is dependent on the immediate mesh geometry, contact ratio, and tooth geometry. The TCA (tooth contact analysis) and elastic influence coefficients are the sources of this kernel.

2.3. Static transmission error and dynamic transmission error

When subjected to load, the deflection of elastic teeth, the distribution of load among multiple pairs, and the compliance of supports modify the contact locus and transmission error (TE). The static transmission error (STE) represents the quasi-static TE that occurs under a gradually changing load, while the dynamic transmission error (DTE) encompasses both inertial and resonant influences. [14]

STE under load is represented as:

$$STE = STE_{angle} \times r_b, \quad (5)$$

and

$$STE_{angle} = i\Delta\theta_g - \Delta\theta_p, \quad (6)$$

where $\Delta\theta_g$ denotes the rotation angle of the driving gear, $\Delta\theta_p$ indicates the rotation angle of the driven gear, and i represents the transmission ratio of the gear pair. To provide a clear representation of the error in the gear meshing line, the angular transmission error is typically multiplied by the base circle radius r_b of the driven gear, resulting in the linear transmission error. [15]

Elasticity is generally incorporated through either linear or nonlinear contact stiffness models. Finite element (FE) models of teeth and assemblies yield comprehensive insights into the loaded contact and deflection fields. In optical and vision processes, the geometry obtained from scans in an unloaded state is integrated with boundary conditions and contact models to approximate STE and DTE. It is common practice to validate these estimates against experimental measurements of strain or dynamic TE. [14]

2.4. Image-based measurement methods for gear geometry and camera imaging model and calibration

By giving digital measurements of tooth flanks (profiles and lead), runout, pitch errors, and wear patterns, image processing aids in TE estimate. The article will present the main imaging modalities and the mathematical models that are used to extract the geometry. Image modalities include high-resolution 2D imaging and subpixel edge detection [16], structured-light/phase-shift 3D scanning [17], stereo photogrammetry, laser triangulation [18], point-cloud scanning, and photogrammetric registration [19]. According to recent studies, machine vision and deep learning are being employed more in industrial settings for geometry extraction and fault identification [7].

Lens distortion adjustments are applied to the typical pinhole camera model. In object coordinates, a 3D point $X = \begin{bmatrix} X & Y & Z & 1 \end{bmatrix}^T$ corresponds to picture homogeneous coordinates x through:

$$\lambda \begin{bmatrix} u \\ v \\ 1 \end{bmatrix} = K \begin{bmatrix} R \mid t \end{bmatrix} \begin{bmatrix} X \\ Y \\ Z \\ 1 \end{bmatrix}, \qquad (7)$$

where λ is the projective scale, R and t are the extrinsics, and K is the intrinsic matrix. In calibration, radial/tangential distortion components are often calculated and modelled (e.g. Brown–Conrady). Because many gear applications need the recovery of minor geometric defects on the tooth profile with less than 100 μm precision, accurate calibration is essential [20].

3. TOOTH EDGE DETECTION

Tooth edge detection derived from optical measurements serves as a crucial preprocessing phase that significantly affects the precision of profile extraction and the subsequent estimation of transmission errors [21].

Detecting edges in environments with reflective, translucent, or heavily textured surfaces poses considerable challenges and is frequently addressed by integrating multiple modalities, such as combining structured light depth data with colour images to clarify misleading edges generated by specular highlights [22].

Precise localization of tooth edges in two-dimensional images serves as a low-cost computational cue for: initial pose or preregistration of the gear, identifying regions of interest (ROIs) for comprehensive surface capture, and identifying absent or damaged teeth for quality assurance. Mistakes in edge detection directly affect registration and deviation calculations, thus making resilience to noise, specular reflections, and minor machining marks crucial. [7]

In classical image processing, two key operators are recognized: Sobel and Canny. Sobel approximates the gradient of an image using small convolution kernels (first derivative). It is efficient and simple, yet it is vulnerable to noise and the selection of thresholds. Sobel is effective as a pre-processing step (for example, in ridge enhancement), but it seldom achieves the required subpixel accuracy independently. Canny, in contrast, is the preferred classical method for robust edge detection. It provides improved localization and noise reduction in comparison to Sobel and is frequently employed as the benchmark in industrial inspection processes. The adjustment of parameters (such as Gaussian sigma and the two thresholds) is crucial and is commonly automated via adaptive thresholding or Otsu-based methods in industrial settings. [20]

Certain techniques generate orientation-sensitive gradient fields that integrate local derivative data with either learned or manually designed structure tensors. These methods generally exhibit greater resilience to variations in texture and shading compared to basic Sobel filters. Deep-learning-based edge detectors, such as HED, RCF, and more contemporary CNN/transformer-based detectors, yield high-quality edge detection and frequently function with subpixel precision when paired with refinement modules. In the context of gear inspection, deep learning techniques have been employed to mitigate specular highlights and to differentiate tool marks from functional edges. Nonetheless, these methods necessitate annotated training data that accurately reflects the gear surfaces and the conditions of illumination. [7]

Achieving sub-pixel localization of the involute profile and the boundaries of the tooth root is essential in metrology [23].

4. EXPERIMENTAL METHODS

In recent years, non-contact optical and vision-based measurement technologies have developed as effective alternatives to conventional contact metrology for inspecting gear tooth flanks. These technologies provide high-resolution and full-surface data acquisition appropriate for subsequent transmission-error (TE) estimation and diagnostic monitoring.

A line-structured-light sensor, in conjunction with a high-precision air-floating rotary table, is capable of acquiring over 1.5 million 3D points on one side of a gear in less than 5 seconds — facilitating the extraction of profile error, pitch error, and tooth flank error from the resultant point cloud [19].

Complementing this, the study "A method for enhanced polymer spur gear inspection based on 3D optical metrology" (2021) applied structured-light 3D

scanning to spur gears, comparing areal optical measurements with traditional coordinate-measuring machine (CMM) methods. It showed that entire flank geometries (beyond a single profile line) can be captured efficiently and that uncertainty remains comparable to tactile methods [24].

More intricate types of gears have also been considered. Lu et al. introduced a three-phase algorithm designed to align 3D scans with the nominal CAD model, reconstruct the actual tooth surface, and measure deviations in the tooth surface on orthogonal face gears, demonstrating that non-contact optical scanning is capable of managing non-standard geometries that can go beyond simple spur or helical gears [25].

These optical techniques are appealing for estimating tooth meshing (TE) because they allow for the digitization of the complete surface geometry of each tooth flank, encompassing involute profile, helix deviation, lead, pitch, runout, and micro-surface irregularities, using sufficiently dense point clouds or meshes. A high point density (for instance, millions of points per flank) guarantees that minor deviations, such as pitch error, profile error, lead error, or flank runout, which affect TE under load, can be accurately captured.

The investigation performed by Li et al. [26] reveals that the experimental outcomes show that, relative to the standard three-step phase-shifting (3-PS) technique, the recommended method provides considerable advancements in phase prediction accuracy, three-dimensional reconstruction precision, dynamic error correction proficiency, and uncertainty estimation. The schematic representation of the FPP system is illustrated below, featuring a camera, a projector, and the object to be measured. This work offers a practical and efficient technical solution for dynamic gear measurement based on fringe projection.

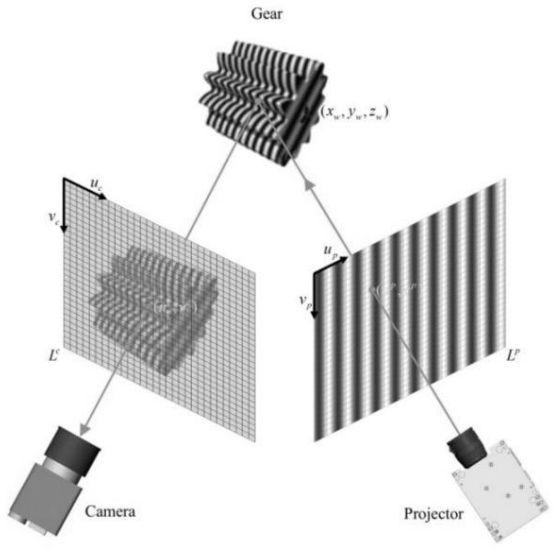

Fig. 1. *FPP-gear measuring system [26]*

Sun et al. [27] present a laser-triangulation method utilizing a line laser model, enhancing pose calibration through a polyhedral artifact, and offering the potential for precise and efficient 3D surface reconstruction, which is appropriate for gear measurement. This indicates that optical gear measurement technology is still undergoing active development, which is crucial since accuracy, speed, and automation are essential for industrial TE estimation or inline inspection.

When applying these techniques in practice, it is essential to take into account several significant experimental factors. First and foremost, calibration and alignment: it is crucial to achieve precise geometric calibration of the scanner, whether it employs structured light or a laser line, and to ensure accurate registration of the gear within the scanning coordinate system. This is vital to verify that the reconstructed point clouds faithfully represent the nominal geometry. In the realm of face-gear scanning research, aligning the scanned point cloud with the design model required the matching of features such as top-land surfaces, circle centers, and tooth surfaces through a multi-stage alignment algorithm [25].

5. IMAGE-PROCESSING, MACHINE LEARNING AND DEEP LEARNING

In recent years, machine learning (ML) and deep learning (DL) have started to assume a significant role, particularly in defect detection, wear monitoring, and image-based gear quality assessment. These techniques could be modified to aid in TE estimation by emphasizing deviations, forecasting wear progression, or even learning correlations from surface geometry or images to TE-related metrics.

An example of this is the work by Xu et al. [28], which advances from 2D images to 3D. The authors developed a deep-learning network that analyzes point-cloud representations of gear components to effectively classify various types of defects (such as fractures, pitting, wear, glue, etc). This indicates that point-cloud deep learning, as opposed to solely relying on 2D imaging, may become essential in gear metrology and quality control, potentially encompassing TE-related geometry analysis.

In a broader sense, recent surveys [29] indicate that deep fully convolutional networks (FCNs) can effectively identify surface defects in components characterized by complex geometries. Even though it does not directly target gears, their research reveals that segmentation networks can adjust to irregular shapes and complicated surfaces, which is advantageous for investigating gear flanks where tooth surfaces lack flatness and consistency. Moreover, the challenge of data scarcity, a continual obstacle in industrial machine learning for gear inspection, is being addressed through the implementation of generative models.

Researchers have utilized a Deep Convolutional Generative Adversarial Network (DCGAN) to synthetically enlarge a constrained dataset of components, not solely gears, and subsequently trained a convolutional neural network (CNN) based on VGG-11 with these synthetic images. The resulting model achieved an F_1-score of 98.40%, demonstrating that GAN-based data augmentation can considerably mitigate the difficulties associated with limited sample sizes that are common in industrial inspection [30].

From the perspective of tribological engineering analysis, such machine learning and deep learning methodologies offer valuable tools for defect detection, which will influence TE over time, facilitate surface condition monitoring throughout the lifespan of components, allowing for the identification of TE changes due to wear, and enable the automation and scaling of inspections in both production and maintenance settings, as well as data-driven mapping from surface geometry or imaging data to TE-relevant metrics.

In a more comprehensive context, the integration of machine learning and deep learning in gear inspection and maintenance is consistent with the trends highlighted in recent literature: a shift from manual, contact-based, or sampling-based inspection methods towards automated, non-contact, image-based, or point cloud-based full-part inspection.

Ari et al. [31] describe a vision system ready for production lines: gears are moved on a rotary table, and their surfaces are continuously monitored by cameras, with defective gears being automatically sorted out using a pneumatic actuator.

In the paper by Yuan et al. [32], median filtering is employed to address impulse noise, while bilateral filtering is utilized to maintain edges in range images. In the context of point clouds, statistical outlier removal and radius-based filtering are often employed.

Surface normal estimation is usually determined for each point to support later segmentation and curvature estimation. Enhanced normal estimation results in superior registration and profile fitting [33].

The occurrence of pitting and spalling alters the surface texture (micro-relief), which can be identified using local binary patterns, GLCM texture features, or morphological filters applied to high-resolution images. Common sources include microscopy and profilometry [25].

Discontinuities in flank contours, derived from profiles or range images, are caused by broken teeth or significant profile deviations. Techniques such as edge detection, Hough-type analysis, or curve-fitting residual analysis prove to be beneficial [34].

The study conducted by Hinz et al. evaluates fringe projection systems over different scale ranges by placing and scanning a calibrated sphere within a high-resolution grid, and aligning the point cloud to gear-centric coordinates [35].

Shi and Sun make use of fast laser-line scanners or structured-light single-shot systems to obtain partial flank scans during the process [36].

Chang et al. implement ML-driven segmentation to isolate the tooth region and recognize anomalies, including pitting and spalling [37].

According to Gorgels and Finkeldey, for the identified areas, it is advisable to seek a route towards more precise measurements or to conduct offline virtual TE calculations [38].

Authors including Tsai and Tsai [39], Tharmakulasingam [40], along with numerous recent studies, demonstrate that 3D finite element modeling, which incorporates elastic tooth-body deformation and multi-tooth contact, provides precise STE predictions that align with experimental rig measurements, provided that all boundary conditions are accurately represented.

Montoya-Zapata et al. [41] conclude that attaining consistent and rapid alignment to the gear center in automated lines remains a relatively undeveloped engineering challenge, particularly concerning helical and non-circular gears.

Li et al. [42] illustrate that deep neural networks can be effectively trained to directly retrieve the absolute phase from a distinctive fringe image that incorporates spatially multiplexed fringe patterns of varying frequencies. The phase that is extracted is free from the spectrum-aliasing problem, which is difficult to avoid in traditional spatial-multiplexing approaches.

6. CONCLUSIONS

Recent innovations in optical metrology, image processing, and machine-learning strategies have transformed the methodologies for measuring, modelling, and interpreting gear transmission error (TE).

While traditional mechanical and encoder-based TE measurement techniques remain critical benchmarks, present non-contact methods, ranging from high-resolution 2D imaging and structured-light scanning to laser triangulation, interferometry, and dense point-cloud reconstruction, now provide thorough, high-fidelity representations of tooth geometry and wear.

These modalities allow for virtual TE computation, improved localization of error sources, and more extensive diagnostic capabilities than previously possible. Edge-detection algorithms, calibration methods, and geometric reconstruction frameworks continue to determine the precision and reliability of image-derived TE estimation.

Meanwhile, machine learning and deep learning are emerging as significant tools for defect detection, wear progression analysis, point-cloud interpretation, and data-driven forecasting of TE related metrics.

ACKNOWLEDGEMENTS

The research was funded by the Ministry of Education and Research of Romania.

REFERENCES

[1] Gregory R.W., Harris S.L., Munro R.G., *A Method of Measuring Transmission, Error in Spur Gears of 1:1 Ratio,* Journal of Scientific Instruments, 40, 1960, 5-9;

[2] Garambois P., Perret-Liaudet J., Rigaud E., *NVH robust optimization of gear macro and microgeometries using an efficient tooth contact model*, Mechanism and Machine Theory, 117, 2017, 78-95;

[3] Palermo A. et al., *The measurement of Gear Transmission Error as an NVH indicator: Theoretical discussion and industrial application via low-cost digital encoders to an all-electric vehicle gearbox*, Mechanical Systems and Signal Processing, 110, 2018, 360-389;

[4] Miura Y. and S. Nakamura, *Gear rattling noise analysis for a diesel engine*, European conference on vehicle noise and vibration, 1998, 3-11, ISSN 1356-1448.

[5] Yu B. et al., *A Virtual Measurement Method of the Transmission Error Based on Point Clouds of the Gear*, Measurement Science Review, 22, 2022, 92-99.

[6] Qin Y. et al., *Gear Pitting Measurement by Multi-Scale Splicing Attention U-Ne*t, Chinese Journal of Mechanical Engineering, 36, 2023, Article number: 50.

[7] Zhang D. et al., *Review on Application of Machine Vision-Based Intelligent Algorithms in Gear Defect Detection*, Processes, 13(10), 2025, 3370.

[8] Allam A. et al., *Detecting Teeth Defects on Automotive Gears Using Deep Learning*, Sensors, 2021, 21(24):8480.

[9] Petrov V. et al., *Advances in Digital Holographic Interferometry*, Journal of Imaging, 2022, 8(7):196.

[10] Litvin F.L. and Fuentes A., *Gear Geometry an Applied Theory – Second Edition (New York: Cambridge University Press), Chapter 9.2,* Cambridge University Press, ISBN 9780511547126.

[11] Kang M. R., Kahraman A., *Measurement of vibratory motions of gears supported by compliant shafts*, Mechanical Systems and Signal Processing, 29, 2012, 391–403.

[12] Barbieri M, Bonori G, Pellicano F, *Corrigendum to: Optimum profile modifications of spur gears by means of genetic algorithms*, Journal of Sound and Vibration, 331, 2012, 4825–4829.

[13] Bejar F. et al., *Review and benchmarking study of different gear contact analysis software in terms of the static transmission error response,* Results in Engineering, 22, 2024.

[14] Zhang J., Lv C. and Li Z., *Investigation of High-Speed Dynamic Transmission Error Testing Using Gear Strain,* Machines 11(10), 956, 2023.

[15] Ji C. et al., *Research on Quasi-Static Transmission Error Measurement of Spur Gears Based on the Acceleration Method*, Machines, 13(10), 941, 2025.

[16] Moru D. and Borro D., *A machine vision algorithm for quality control inspection of gears*, The International Journal of Advanced Manufacturing Technology, 2019, 106, 105–123.

[17] Shang Z. et al., *Measurement of gear tooth profiles using incoherent line structured light*, Measurement, 189, 2022.

[18] Luo M. and Zhong S., *Non-Contact Measurement of Small-Module Gears Using Optical Coherence Tomography*, Appl. Sci., 2018, 8(12), 2490.

[19] Guo X. et al., *3D measurement of gears based on a line structured light sensor,* Precision Engineering, 61, 2020, 160-169.

[20] Major M. et al., *Evaluation of a Structured Light Scanner for 3D Facial Imaging: A Comparative Study with Direct Anthropometry*, Sensors, 24(16), 5286, 2024.

[21] Chen Y.-C., Chen C.-J. and Hsiao C.-Y., *Optical inspection system for gear tooth surfaces using a projection moiré method.,* Sensors, 19(6), 1450, 2019.

[22] Pillarz M. et al., *Gear Shape Measurement Potential of Laser Triangulation and Confocal-Chromatic Distance Sensors,* Sensors, 21(3), 937, 2021.

[23] Onyedinma E. G. et al., *Exploring the Effectiveness of Sobel, Canny, and Prewitt Edge Detection Algorithms on Digital Images,* World Journal of Advanced Engineering Technology and Sciences, 15(1), 2025, 1722-1730.

[24] Urbas U. et al., *A method for enhanced polymer spur gear inspection based on 3D optical metrology,* Measurement, 169, 108584, 2021.

[25] Lu X. et al., *A Measurement Solution of Face Gears with 3D Optical Scanning,* Materials, 15(17), 6069, 2022.

[26] Li Z. et al., *Deep learning-based dynamic error correction and uncertainty estimation for digital twin-assisted fringe projection profilometry of rotating gears,* Jiangxi University of Science and Technology, DOI: https://doi.org/10.48550/arXiv.2512.00859, 2025.

[27] Sun Y. et al., *Line Laser 3D Measurement Method and Experiments of Gears*, Photonics, 12(8), 782, 2025.

[28] Xu Z. et al., *Defect detection of gear parts in virtual manufacturing*, Visual Computing for Industry, Biomedicine, and Art, 6:6, 2023.

[29] Peña D.G. et al, *Exploring deep fully convolutional neural networks for surface defect detection in complex geometries,* The International Journal of Advanced Manufacturing Technology,134, 2024, 97–111.

[30] Gao H. et al., *A Deep Convolutional Generative Adversarial Networks-Based Method for Defect Detection in Small Sample Industrial Parts Images,* Appl. Sci., 12(13), 6569, 2022.

[31] Ari P.D, Akkoyun F., Ercetin A., *A Machine Vision System for Gear Defect Detection,* Processes, 13(6), 1727, 2025.

[32] Yuan H. et al., *Research on the Improved ICP Algorithm for LiDAR Point Cloud Registration,* Sensors, 25(15), 4748, 2025.

[33] Zhan X. et al., *A point cloud registration algorithm based on normal vector and particle swarm optimization,* Measurement and Control, 53, 3-4, 2020.

[34] Miao J. et al., *Vision measuring method for the involute profile of a gear shaft,* Applied Optics, 59 (13), 2020, 4183-4190.

[35] Hinz L. et al., *Fringe Projection Profilometry in Production Metrology: A Multi-Scale Comparison in Sheet-Bulk Metal Forming,* Sensors, 21(7):2389, 2021.

[36] Shi Z. and Sun Y., *An overview on line laser 3D measurement of gears*, Precision Engineering, 88, 2024, 823-844.

[37] Chang H., Borghesani P., Peng Z., *Automated assessment of gear wear mechanism and severity using mould images and convolutional neural networks,* Tribology International, 147, 2020, 106280.

[38] Gorgels C. and Finkeldey M., *Finding the Right Task for Optical Gear Metrology,* Gear Technology, November/December 2023, 53-59.

[39] Tsai M.-H., Tsai Y.-C., *A method for calculating static transmission errors of plastic spur gears using FEM evaluation,* Finite Elements in Analysis and Design, 27 (4), 1997, 345-357.

[40] Tharmakulasingam R, *Transmission Error in Spur Gears: Static and Dynamic Finite-Element Modeling and Design Optimization*, London: School of Engineering and Design Brunel University, Doctoral Thesis, 6-50.

[41] Montoya-Zapata D. et al., *Dimensional inspection of spur and helical gear teeth manufactured by Laser Metal Deposition,* Procedia CIRP, 124, 2024, 223–226.

[42] Li Y. et al., *Deep-learning-enabled dual-frequency composite fringe projection profilometry for single-shot absolute 3D shape measurement*, Opto-Electronic Advances, 5(5), 210021, 2022.